frontiers | Frontiers in Earth Science

TYPE Original Research
PUBLISHED 15 December 2023
DOI 10.3389/feart.2023.1281076

OPEN ACCESS

EDITED BY
Susanne Maciel,
University of Brasilia, Brazil

REVIEWED BY
Rejane Ennes Cicerelli,
University of Brasilia, Brazil
Marcelo Rocha,
University of Brasilia, Brazil

*CORRESPONDENCE
Leonides Guireli Netto,
leonidesnetto@ipt.br

RECEIVED 21 August 2023
ACCEPTED 05 December 2023
PUBLISHED 15 December 2023

CITATION
Guireli Netto L, Singha K, Moreira CA, Gandolfo OCB and Albarelli DSNA (2023), Investigation of fractured rock beneath a uranium-tailing storage dam through UAV digital photogrammetry and seismic refraction tomography.
Front. Earth Sci. 11:1281076.
doi: 10.3389/feart.2023.1281076

Investigation of fractured rock beneath a uranium-tailing storage dam through UAV digital photogrammetry and seismic refraction tomography

Leonides Guireli Netto[1,2]*, Kamini Singha[3], César Augusto Moreira[1], Otávio Coaracy Brasil Gandolfo[2] and Daniel Seabra Nogueira Alves Albarelli[2]

[1]Geosciences and Exact Sciences Institute (IGCE), São Paulo State University (UNESP), Rio Claro, Brazil, [2]Cities, Infrastructure and Environment Department, Institute for Technological Research (IPT), São Paulo, Brazil, [3]Geology and Geological Engineering Department, Colorado School of Mines, Golden, CO, United States

Failure events in dams can be associated with processes in the dam body and in the foundation of the structure. If they are properly identified in early stages, corrective actions can take place, leading to a reduction in the risk of collapse and/or rupture of the dam. Most studies on dams are carried out on the body of the dam; however, problems associated with the foundation of the structure can also lead to loss of stability and subsequent ruptures. This study presents an analysis of the advantages and limitations of the use of seismic refraction in hydrogeological studies of fractured aquifers under pressure from large loads, specifically a dam in this case. Seismic refraction data were collected on an outcrop of fractured rock near a uranium storage dam foundation in southeastern Brazil. The results and interpretations were supported by a structural analysis performed through manual strike measurements collected with a Clark compass and an uncrewed aerial vehicle digital photogrammetry survey in an outcrop. The digital photogrammetric survey mapped the spatial distribution and orientation of the geological structures of the rock mass. Although the structural measurements performed through digital photogrammetry presented greater variability than the measurements collected from the compass, the maximum density of the fracture measurements obtained from both methods were similar and were corroborated by the regional and local fracture patterning. The integration of seismic refraction data with geotechnical and geological investigations allowed us to identify the positioning of structural lineaments in the rock mass and zones with a higher degree of rock alteration. The identification of highly fractured zones in the rock mass from such non-invasive investigations could be used to assist in decision making for structural reinforcements in the foundation of the dam to avoid the loss of stability at the foot of the dam from possible leaks or water flows from the reservoir.

KEYWORDS

dam foundation, geophysics, uranium, seismic refraction, UAV

1 Introduction

Dams create artificial reservoirs for the accumulation of materials in a liquid or pasty state. These structures are built transverse to the flow direction of a watercourse and are classified in relation to the material used in the construction: earth, concrete, mining tailings and rockfill. The use of dams was crucial in the development of human history due to the need to store water, which can later be used for agriculture, domestic use, and energy generation (Kirchherr and Charles, 2016; Wu et al., 2019). Dams are also constructed to manage material from mineral exploration around the world (Schoenberger, 2016; Islam and Murakami, 2021). The number of dam investigation studies has grown considerably in recent years, especially in countries with a large mineral economy (Habel et al., 2020; Dimech et al., 2022; Chen et al., 2023). In Brazil, for example, one of the main mining countries in South America, there has been an increase in geophysical and geotechnical studies on dams after the recent ruptures of tailing dams (Koppe, 2021; Moreira et al., 2022). The growth in the number of studies may also be correlated with the global increase in catastrophic failures of mine tailings dams in recent years (Owen et al., 2020). In addition to human, social and economic losses, possible land and water contamination from the rupture of tailings dams motivate actions to prevent and control their failure (Lottermoser, 2010; Rotta et al., 2020).

Many dams, especially behind the large water reservoirs of the last century, were built without a complete understanding of the possible geotechnical problems that could occur in the foundations (Schuster, 2006). An older survey of 1,620 dam in Spain during 1799 and 1944 studied the main causes of the 308 ruptures of these structures in that period. It was observed that in 40% of the dam failures the problems were caused by deficiencies of the foundation (Jansen, 1983). More recently, a survey conducted by the Association of State Dam Safety Officials between 2010 and 2019 showed that foundation problems, including settlement and slope instability, caused about 30% of all dam failures in the U.S. (ASDSO, 2023). In concrete dams, 80% of ruptures were caused by overtopping or problems from internal erosion in the foundation (Zhang et al., 2016). One of the main problems in designing a dam is to provide sufficient stability to prevent the structure from sliding failure. The design can become complex when there are several weak structural planes in the dam foundation (Xuhua et al., 2008). The load of the stored material, complicated geology, and the weakening of the rock mass over the years are just some of the factors that motivate studies directed at the foundation of the dams (Asthana and Khare, 2022). In view of the complexity of the problem and the potentially catastrophic impact of dam failures, studies focused on obtaining geological and geotechnical information on the rock mass of dams' foundation are important (Sari et al., 2020).

Although investigations into dams have grown in the last decade, most studies have focused on investigating the body of the dam to identify leakage zones in compacted soil and mining tailings structures or detect cracks in the face of concrete, for example, (Maalouf et al., 2022; Oliveira et al., 2023; Srivastava et al., 2023). Many of these studies seek to identify zones of water percolation, which can alter the physical stability of the dam and lead to a failure of the structure (Sentenac et al., 2017; Camarero et al., 2019; Guireli Netto et al., 2020b; Arcila et al., 2021). However, other important areas of dams are less frequently investigated in detail, including the dam foundation or contact zones between different materials, such as the contact between soils and concrete used in earth and rockfill dams, tunnels and coastal levees (Liu et al., 2021) or between the concrete slab and the dam body of concrete-faced rockfill dams. The identification and monitoring of certain geological elements are also directly related to the stability of the dam. Faults, fractures, erosion channels or cavities sometimes cannot be completely removed from the foundation in rock masses prior to the construction of the dam (Fell et al., 2005). Deficiencies can facilitate the creation of voids and facilitate the flow of water and material carriage from the dam body at these points (Zhang et al., 2004). Geotechnical instruments such as piezometers, inclinometers, settlement gauges, water level and flow meters are often used, but usually provide point values strictly from the place where the instruments are installed (Fell et al., 2005). Geophysical methods, in contrast, can be a spatially exhaustive, non-invasive investigation alternative to complement such direct tools (Sastry and Chahar, 2019; Guireli Netto et al., 2020a; Guo et al., 2022). In addition to the well-established use of electrical methods on dams, there has been an increase in the use of seismic methods (Bedrosian et al., 2012; Guedes et al., 2023). Most methods have been performed in the top of the crest region and on the downstream slope of the dam to identify zones with compaction arising from soil disintegration due to water flow (Cardarelli et al., 2014; Guireli Netto et al., 2020b).

Between 1906 and 1939, the total world extraction of radium was about 1,000 g and that of uranium approximately 4,000 tons (t) (Yemel'yanov and Yevstyukhin, 1969), and the search for radioactive minerals was fostered mainly to supply the war industry and the production of nuclear energy (Eidemüller, 2021). By 1960, annual uranium oxide production in the U.S. reached 15,000 t, 13,000 t in Canada, more than 6,000 t in South Africa, 1,000 t in the Republic of Congo and Australia, and 750 t in France (Eidemüller, 2021). Nuclear power emerged as an important element of any sustainable solution to meet energy needs given increasing energy demand due to the growth of the global population and an increasing emphasis on low-carbon technologies (Wang et al., 2023), resulting in additional radioactive mineral mines in several countries. Besides the challenges linked to the decontamination and environmental recovery of facilities where radioactive materials have been discarded, mining has several environmental liabilities. These liabilities, such as dams, tailings piles, and radioisotope retention ponds, need to be monitored for physical integrity of the structure (Owen et al., 2020; Rotta et al., 2020).

The present study carried out a structural survey in a fractured rock mass near the foot of a radioactive material storage dam. Here, we used digital photogrammetry to determine where bedrock fractures were located near a dam using uncrewed aerial vehicle (UAV) images. Data were compared to manual strike measurements collected with a Clark compass at the outcrop, and seismic refraction tomography was collected close to rock mass of the dam foundation. Refraction seismic tomography is not a technique commonly used in studies of dam investigations, especially focusing on the foundation of the structure. This study looks to provide advantages and disadvantages in the evaluation of hydrogeological changes caused by the accumulation of large loads related to the material stored on fractured rock masses given integrated, non-invasive data. Identification of fracturing in dam foundations without the need for

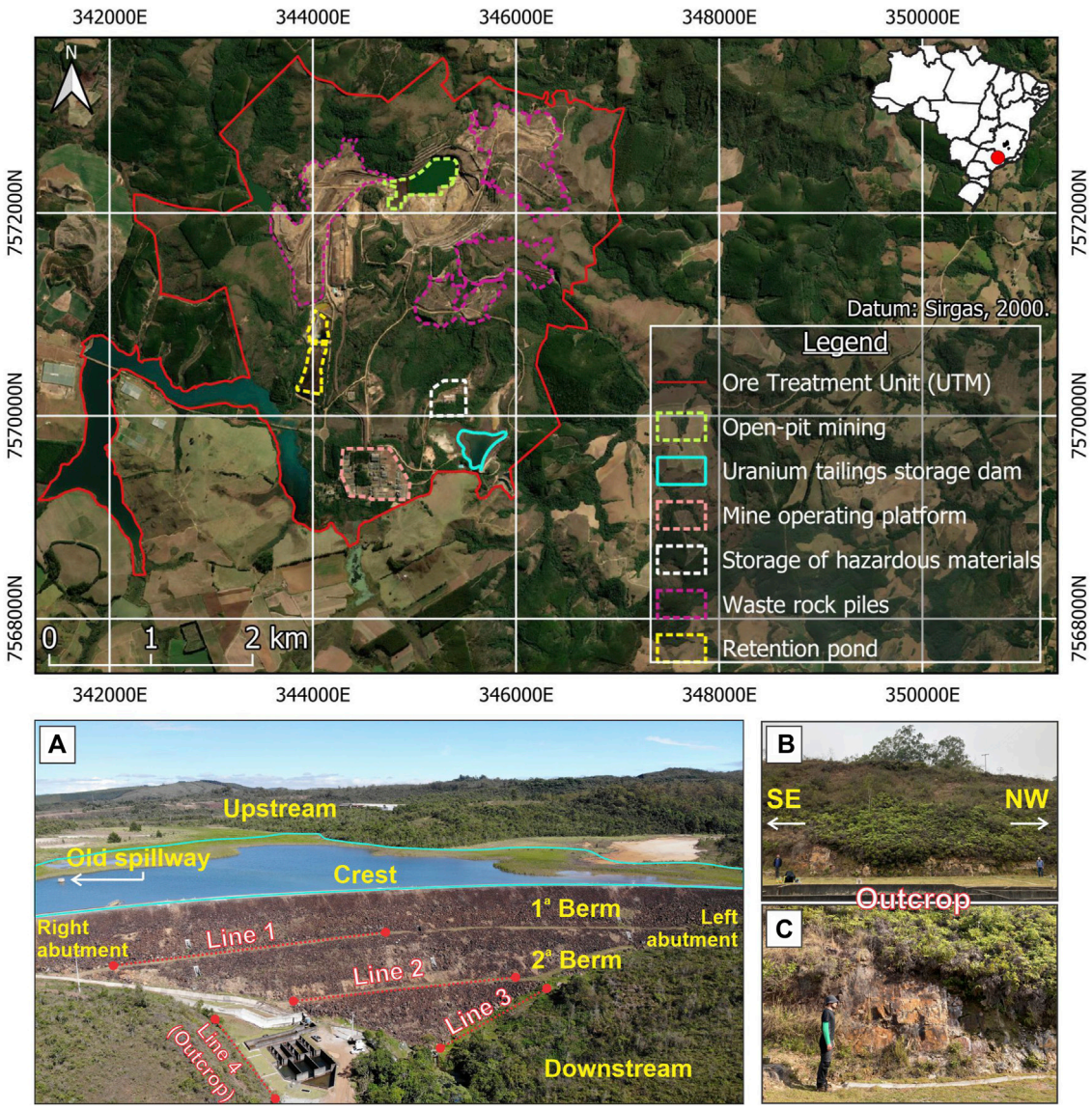

FIGURE 1
Overview of Ore Treatment Unit, including **(A)** locations of the tailings storage dam, **(B)** outcrop used for structural data acquisition and the seismic acquisition lines in the study area where **(C)** shows the rock mass outcropped in detail, scale: 1.77 m high. Datum: Sirgas, 2000.

invasive investigations to the structure is desirable, especially in old structures where updated geotechnical information may be absent or in structures with high risk or consequences of rupture.

2 Study site

2.1 Location and historical use

This project explores a dam within the Industrial Mining Complex of Poços de Caldas, currently known as the Ore Treatment Unit, located in the southwest region of the State of Minas Gerais in the municipality of Caldas, Brazil, with an area of 15 km^2 (Figure 1). The main activities carried out by the Industrial Mining Complex were the mining and processing of uranium ore. The Osamu Utsumi mine is part of the Industrial Mining Complex of Poços de Caldas and was the first mine to produce yellow cake (uranium concentrate) in Brazil, used as raw material to produce nuclear fuel. Mining activities at Osamu Utsumi mine began in 1977 with the opening of an open pit mine. The installation operated discontinuously until 1995, with a total production of 1030t U_3O_8 (Cipriani, 2002). Osamu Utsumi mine's uranium processing and extraction plant was designed to treat approximately 750,000 t/year of ore. During the 11 years of operation, around 2.3 Mt of ore were mined (Filho, 2014). It was estimated that 94.5 Mt of rock and soil were removed during the operation of Ore Treatment Unit and that only 2% of that amount was sent to processing (Cipriani, 2002). The rest of the material, around 89 Mt, was disposed in open-air waste piles (Figure 1). The first waste dump was built in 1981. At the end of operations, the Osamu Utsumi mine had four waste dumps. In addition to this material, 2.1 tons of

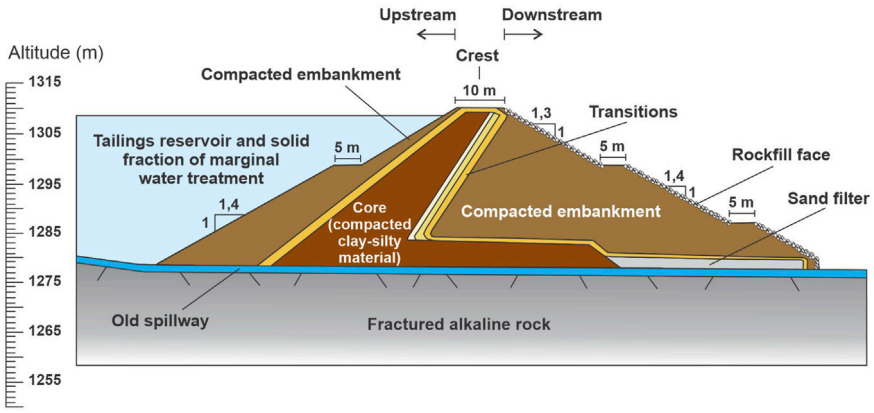

FIGURE 2
Schematic of the cross-section of the tailings dam of the Osamu Utsumi mine with details of the geometry and materials used in the construction of the dam.

depleted ore were disposed in the tailings dam, after being crushed and leached at the processing plant (Geração controlada com destinação segura disposição total a seco, 2019, p.24).

2.2 Characteristics of the radioactive material storage dam

The tailings storage dam in this study is located in the southeast region of the mine (Figure 1). The dam was built in the early 1980s and has a real volume capacity of 1 million m^3. During the operation phase, approximately 4.8 TBq (130 Ci) of 238U, 15 TBq (405 Ci) of 226Ra and 4.2 TBq (112 Ci) of 228Ra were discharged into its reservoir. Since 1995, after the closure of Ore Treatment Unit operations, the reservoir has not received tailings. The most recent studies showed that the dam stores around 2.1 tons of depleted ore (Geração controlada com destinação segura disposição total a seco, 2019, p.24). This material was crushed and leached at the processing plant and the result was waste with low uranium content. The reservoir also stores 0.1 tons of solid fraction from the treatment of marginal waters. The liquid effluent from the processing plant was treated and the resulting solids were released in the form of pulp in the tailings basin (Geração controlada com destinação segura disposição total a seco, 2019, p.24).

The dam body consists of a compacted rockfill massif and a clayey core inclined upstream (Figure 2). The 435-m long structure has a curved axis with a 380-m radius, with concavity facing downstream, and two building levels visible downstream and a 42 m maximum height (Figures 1, 2). The dam has a system of filters and transitions between the clayey core and the upstream and downstream rockfills, both connected to a horizontal drainage mat (Figure 2). This hydraulic system captures the water percolated by the dam body and foundation and transports it downstream in a controlled manner, where it is collected through passage boxes and sent to a system of baffles. During a few years of operation, the dam had a tulip-type spillway. This structure was connected to a concrete gallery installed under the dam body. Water was transported downstream through free-flowing concrete pipes (old spillway in blue in Figure 2) (Arcila et al., 2021). The inactivated structure was concreted for waterproofing. However, the existence of water stored inside this hydraulic structure that can infiltrate the rock mass of the foundation cannot be ruled out.

3 Geological and geotechnical context of osamu utsumi mine

The geological context of the site is strongly influenced by Poços de Caldas Plateau. The plateau is inserted between the limits of the States of São Paulo and Minas Gerais and has the shape of a dome, which has on its edges escarpments of faults. This fracturing pattern was observed in the crystalline bedrock (Figure 3; Biondi, 1976). The Poços de Caldas Plateau has two large fault systems with predominant directions N40E and N60W (Fraenkel et al., 1985). Faults and fractures occur throughout the alkaline complex and extend through the country rocks with the same predominant directions (Almeida Filho and Paradella, 1977; Magno Júnior, 1985). This orientation of fracturing is observed throughout the Plateau. Thus, the structural context of the Osamu Utsumi mine is the main control on the hydrogeology in the area. The two large systems of deep faults favored the percolation and infiltration of water in the rock massif (Fraenkel et al., 1985).

The first geological-geotechnical mapping of the mining area was carried out by the Institute of Technological Research of the state of São Paulo (Instituto de Pesquisas Tecnológicas – IPT, 1977) and aimed to determine the spatial distribution of the strata along the area of the mine pit, as well as to determine the physical properties of these geological materials. The geotechnical description was based on drill core samples, geophysical prospecting and laboratory tests of materials in the Osamu Utsumi mine pit. Three primary lithologies found were classified.

- Alluvium: deposits consisting mostly of clay minerals and gravel with organic matter. Restricted to the valleys in the mine area.
- Alkaline rock soil: feldspathic and clayey soil, resulting from alteration of the local rock under physical and chemical weathering.
- Bedrock: consisting of alkaline rocks of tinguaite, foiaite and breccia types, with varying fracturing and integrity.

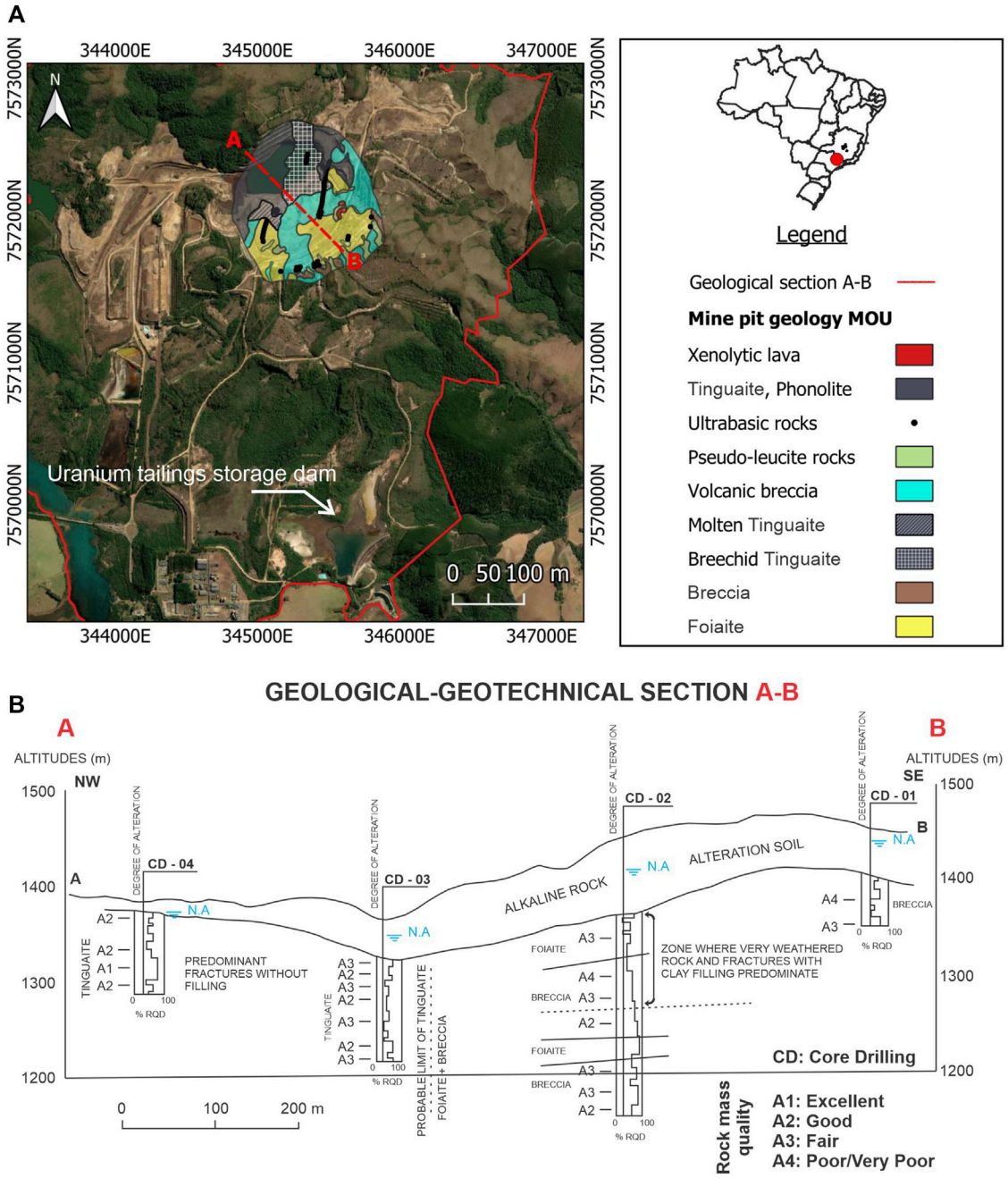

FIGURE 3
(A) Geological map of the Osamu Utsumi mine pit area. **(B)** Geological-geotechnical section of the mine pit in the NW-SE direction obtained from core drillings conducted before the start of mining operations (Instituto de Pesquisas Tecnológicas – IPT, 1977).

Many lineaments were observed, highlighted by the existence of structural lows that developed in the NW and NE directions. Such lineaments, mainly those in the NE direction, coincided with the areas of greatest alteration of the rock mass. Outcrops were observed near the foot of the dam, as well as the presence of boulders. The shallow presence of the rock mass was used to evaluate the ability of seismic refraction tomography to identify changes associated with the rock mass under the dam.

4 Methods

4.1 Seismic refraction tomography (SRT)

Seismic surveys were carried out on the downstream slope of the dam body and in the region of the dam foot (Figure 1A). In the field, seismic waves were generated using a sledgehammer and data were collected using a 24-channel Geode (Geometrics) seismograph. Geophones with a resonant frequency of 10 Hz were used. As this is a shallow investigation

(a few meters deep), the relationship between the depth and the wavelength of the method is crucial for determining the frequencies of the geophones that will provide high-quality responses in the field (Foti et al., 2003). The characteristics of the array (length and position of the lines) and the spacing between the geophones were chosen to obtain the best possible data coverage along the entirety of the lines (Foti et al., 2018). The first arrivals of the P-wave on line 1, for example, show that it was possible to take readings on all geophones when a shot was made at the 9.5 m position. This condition was considered in all acquisition lines (Supplementary Figure S1). Each acquisition line carried out on the berms was 92 m long (Figure 1; lines 1 and 2). The spacing between the geophones was 4 m. The acquisition line carried out at the foot of the downstream slope was half the length of those on the berm (Figure 1, line 3), so a smaller spacing between the geophones was adopted (2 m). The same criterion was adopted in the acquisition on line 4, which was close to the contact zone between dam body and the natural relief; it was 25 m long and had a spacing between the geophones of 1 m (Figure 1, line 4).

Seismic refraction data were processed in Rayfract (by Intelligent Resources Inc.). Geotechnical and engineering geology studies that analyzed seismic refraction data using Rayfract showed that it is feasible to map boulders and rock blocks in compacted soil massifs, especially in acquisition lines with high resolution (Sari et al., 2020; Benjumea et al., 2021). The characteristics of the line acquisition were inserted into the software, such as the initial position of the geophones, the spacing between them, the trigger delay and the topographic details of each geophone. After that, the arrival of the waves in each shot were picked manually for each geophone. The software generated a graph (time *versus* distance), where we could observe whether the measurements were coherent (Supplementary Figure S2). The software's seismic refraction tomography processing then uses the Wavepath Eikonal Traveltime (WET) inversion method of Schuster and Quintus-Bosz (1993), which use the Fresnel volume approach to model propagation of first-break energy in a physically meaningful way (Zelt et al., 2013). WET can be considered an optimized version of the Generalized Reciprocal Method (GRM) algorithm. Rather than using a constant separation of the receiver provided by the user throughout the profile, WET automatically estimates the separation of the local receiver in each geophone from the angles of the direct and reverse waves (Lecomte et al., 2000). Thus, the separation of the receivers obtained may vary laterally along the profile, which explains the success of studies on steep slopes (Capizzi and Martorana, 2014; Tomás et al., 2018). WET inversion was performed on all acquisition lines individually. After the manual determination of the first arrival times of the P-waves and insertion of the acquisition parameters, iterations were performed from the initial model. The highest root-mean-squared error was 1.17 m (line 1) and the lowest was 0.40 m (line 4). Both were satisfactory and showed reliability in data processing. In addition to the low error associated with the model, the software provides a map of the areas of coverage of the seismic rays in relation to depth (Supplementary Figure S3). In all lines the coverage was good. Finally, the result was a tomographic section with P-wave velocities (Vp) obtained from each acquisition.

4.2 Structural surveys: compass and uncrewed aerial vehicle

Structural data were collected from an outcrop located near the foot of the uranium tailings storage dam (Figure 1A). The outcrop is approximately 60 m long and 4 m high and was chosen because the alkaline rock, exposed to physical-chemical weathering, showed well-marked fracturing at sub-horizontal and vertical dip angles (Figure 1B). In addition, regional and local geological surveys carried out in previous studies in the mining area have shown that the rock mass of the foundation was composed of the same lithology as this outcrop. Structural measurements were collected from traditional surveying using a compass and uncrewed aerial vehicle (popularly called a drone). Compass measurements were taken along the entire outcrop at different points with a Clar stratum compass, model GEKOM-PRO, produced by the German company Breithaupt.

A total of 20 measurements were collected for each family of fractures. Due to the dimensions of the outcrop and the number of samples scattered along the rock mass, we expected these measurements to provide a representative sample of the structural behavior of this study location (Figure 1C). The photogrammetric survey was carried out with the Mavic Air drone, model CP.PT.00000165.01, produced by DJI. The drone technical specifications are presented in Table 1. A manual flight was performed in which the drone stops in the air to capture the image and then moves to the next spot to acquire the next image, instead of taking images while moving at an assigned flight height and speed. This procedure reduces the chance of having motion-blurred images. Variable oblique views of the outcrop were preferred to provide better point-cloud resolution and avoid occlusion. The objective in applying the two techniques for acquiring the orientation of fractures and faults was to compare the viability and limitations of indirect data collection such as UAV digital photogrammetry surveys to "hard" data. UAV have been applied in several geological-geotechnical studies of structural mapping of fractured rocks; however, studies proving the compatibility of UAV surveys and traditional structural surveys (using a stratum compass) are still necessary and important (Salvini et al., 2017; Albarelli et al., 2021; Junaid et al., 2022).

The on-board UAV GNSS provided georeferenced images in the WGS 84 coordinate system, allowing the reconstruction of a scaled and orientated 3D model described below (section 5.1). The vertical Datum used was Imbituba, located in the state of Santa Catarina, Brazil. To increase the accuracy of the geolocation of the 3D model, a Trimble Pathfinder 85,340-00 GNSS was used to acquire ten ground control points coordinates during the field work via absolute positioning measurements in the static mode during 5 min for each ground control point. The ground control points coordinates collected were post processed to increase their accuracy using a free online service provided by the Brazilian Institute of Geography and Statistics. This service uses a program called Canadian Spatial Reference System Precise Point Positioning developed by Geodetic Survey Division of Natural Resources of Canada in which the final post-processed coordinates are referenced to the Geocentric Reference System for the Americas - SIRGAS2000 and to the International Terrestrial Reference Frame. The post-processed coordinates of the ground control points ranged from 0.80 m to 2.20 m accuracy for the planimetric (x, y) position and from 1.92 m to 4.55 m accuracy in the altimetric (z) position.

4.2.1 Digital photogrammetry and point cloud generation

A total of 108 images taken by the UAV were used in the photogrammetric software Pix4D mapper version 4.6.4 for the 3D digital model reconstruction of the outcrop as a densified point cloud (Supplementary Figure S4) and textured mesh (Figure 4); the latter is

TABLE 1 Technical specifications drone Mavic Air.

Category	RGB camera
Sensor	Effective Pixels CMOS 1/2,3: 12 MP
Lens	FOV: 85°/35 mm Equivalent Format: 24 mm/Opening: f/2.8/Shot Range: 0.5 ma 8
ISO Range	100–3,200 (manual mode–for pictures)
Image size	4,056 × 3,040 pixels
Photo format	JPEG/DNG (RAW)
Satellite Positioning System	GPS/GLONASS

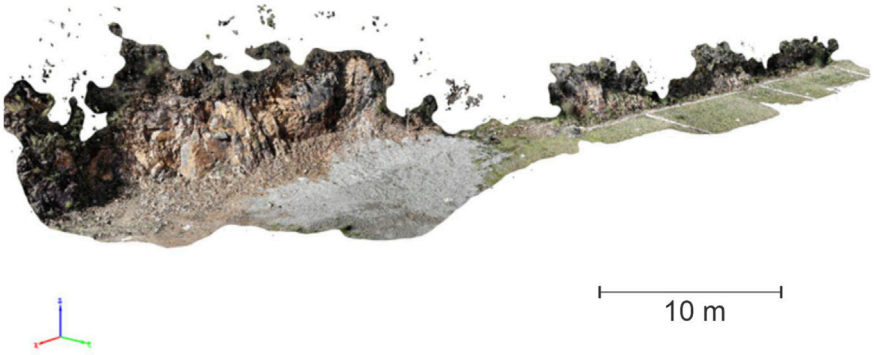

FIGURE 4
Digital outcrop model obtained from digital photogrammetry.

commonly called a digital outcrop model. The standard processing parameters of the 3D model template provided by the software was used to allow a reasonably fast processing time and reliable quality of the point cloud. Moreover, seven ground control points collected in the field campaign were inserted in the model to improve the relative (measurements) and absolute (georeferencing) accuracy of the model reconstruction and three ground control points were used independently as check points to access the absolute accuracy. The main objective of using a 3D model of the outcrop was not to accurately georeference it on the terrain, but rather to acquire structural measurements of fractures comparable with the traditional geological compass.

Because the altimetric (z) precision of the ground control points and checkpoints obtained after the post processing (1.92 m–4.55 m) did not correspond to the reality of the terrain, where horizontal variability was close to zero, the z coordinates inserted for the model reconstruction were all the same to better represent the actual physiographic conditions of the terrain. The densified point cloud has approximately 5 million points, a ground sampling distance of 1.9 mm/pixel, point spacing of less than 1 mm and an average point density of 336,809 points/m^3. This pixel size of 1.9 x 1.9 represents 3.61 square millimeters, which we consider a high spatial resolution for digital outcrop characterization (Albarelli et al., 2021; Junaid et al., 2022). The results from the model absolute accuracy are presented in Table 2.

4.2.2 Discontinuity extraction

The discontinuities on the surface of the outcrop were manually mapped in the point cloud using the Compass plugin (Thiele et al., 2017) in the open-source software CloudCompare v2.12.4 (2023). The Trace tool uses a least-cost path algorithm to automatically connect traces between a start and end point picked by the user (Supplementary Figure S5), and then estimates the orientation of a best-fitting plane to the mapped trace (Supplementary Figure S6). The basic principle of least-cost path analysis is to determine the best interaction routes or corridors on a graph by equalizing cells and pairs of adjacent cells with nodes and arcs (Mundeli and Shirabe, 2021). The software uses an optimized implementation of Dijkstra's algorithm. From five cost functions (Colour Brightness, Colour Similarity, Gradient, Curvature, for example,) different structures and types of geological data, such as fractures and faults, can be mapped (Thiele et al., 2017; Nesbit et al., 2018). The Plane tool allows us to measure surface orientations by applying a least-squares best-fitting plane on a point picked by the user, in this case on the surface of the slope. A total of 61 discontinuities traces and 61 planes on the surface of the outcrop were digitally mapped and measured (Supplementary Figure S8). This number of measurements allowed for a statistical comparison with the measurements collected by the compass. The collected measurements were exported in a table and inserted into OpenStereo (Grohmann and Campanha, 2010).

5 Results and discussion

5.1 Structural geological analysis: digital photogrammetry and compass surveys

The structural analysis of the study area was performed from UAV and compass surveys, focusing on the main fracture families and

TABLE 2 Model absolute accuracy.

	Ground control point errors (m)			Checkpoint errors (m)		
	x	y	z	x	y	Z
Mean	0.01	−0.01	0.00	−0.34	0.05	−0.05
St. Dev	0.46	0.32	0.03	0.90	0.89	0.12
Error RMS	0.47	0.32	0.03	0.96	0.89	0.13

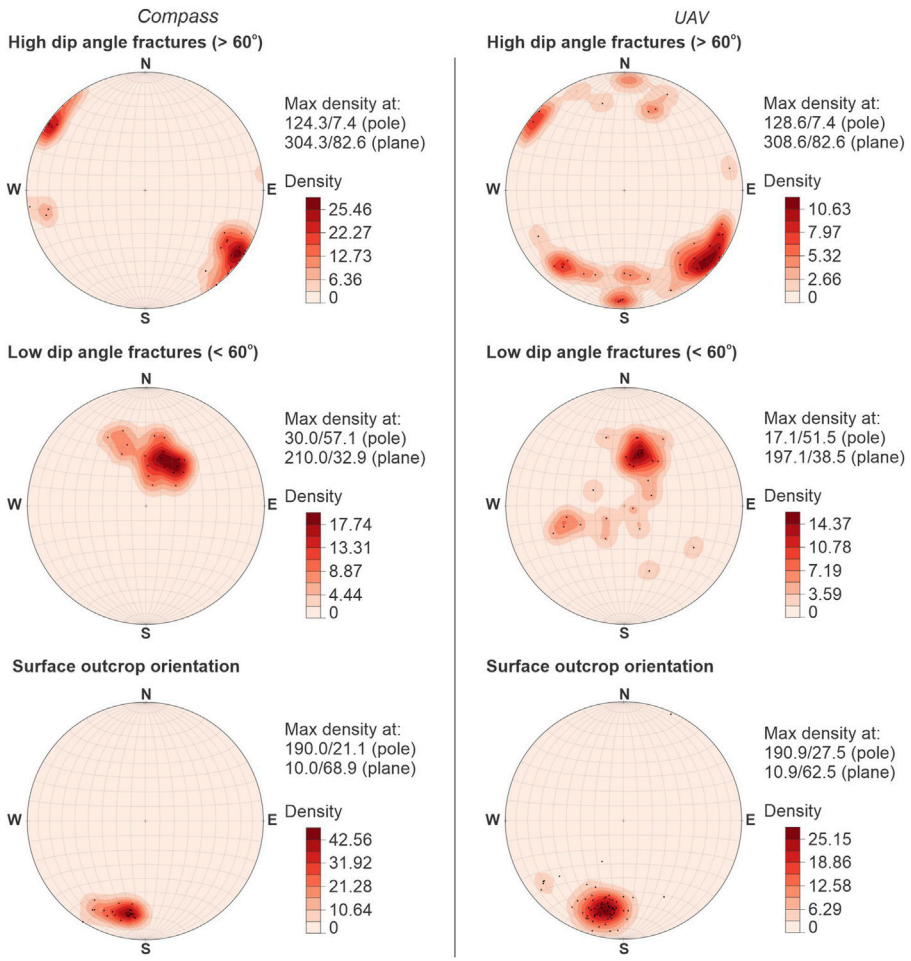

FIGURE 5
Stereograms for analysis and comparison of UAV and compass surveys.

the bedding plane orientation. The fracture families were defined according to the dipping angles: high-dip-angle (>60°) and low-dip-angle (<60°) fractures. The structural data were plotted on a stereogram for analysis and comparison of UAV and compass surveys (Figure 5). Although the UAV data showed greater variability than the compass surveys, the positioning of the maximum density obtained in both surveys are similar and thus suggests reliability of the data measured indirectly using UAV (Figure 5). The high-dip-angle fractures obtained with UAV survey presented a maximum density of 308° for the dip direction. This measurement is corroborated by a regional pattern of faults that shows a dip direction of 290° (Camarero et al., 2021) and NE-SW strike (Almeida Filho and Paradella, 1977; Fraenkel et al., 1985; Almeida, 1986), as well by the local measurements of 290° and 270° obtained in the open pit SE and NE wall of the Osamu Utsumi mine, respectively, from a compass survey by Camarero et al. (2021). The low-dip-angle fractures obtained with UAV presented a maximum density of 197° for the dip direction, corroborated with another regional fault system of NW-SE strike (Almeida Filho and Paradella, 1977; Fraenkel et al., 1985; Almeida, 1986) and local measurements of 200° for dip direction obtained in the open pit NW wall of the Osamu Utsumi mine from a compass survey by Camarero et al. (2021).

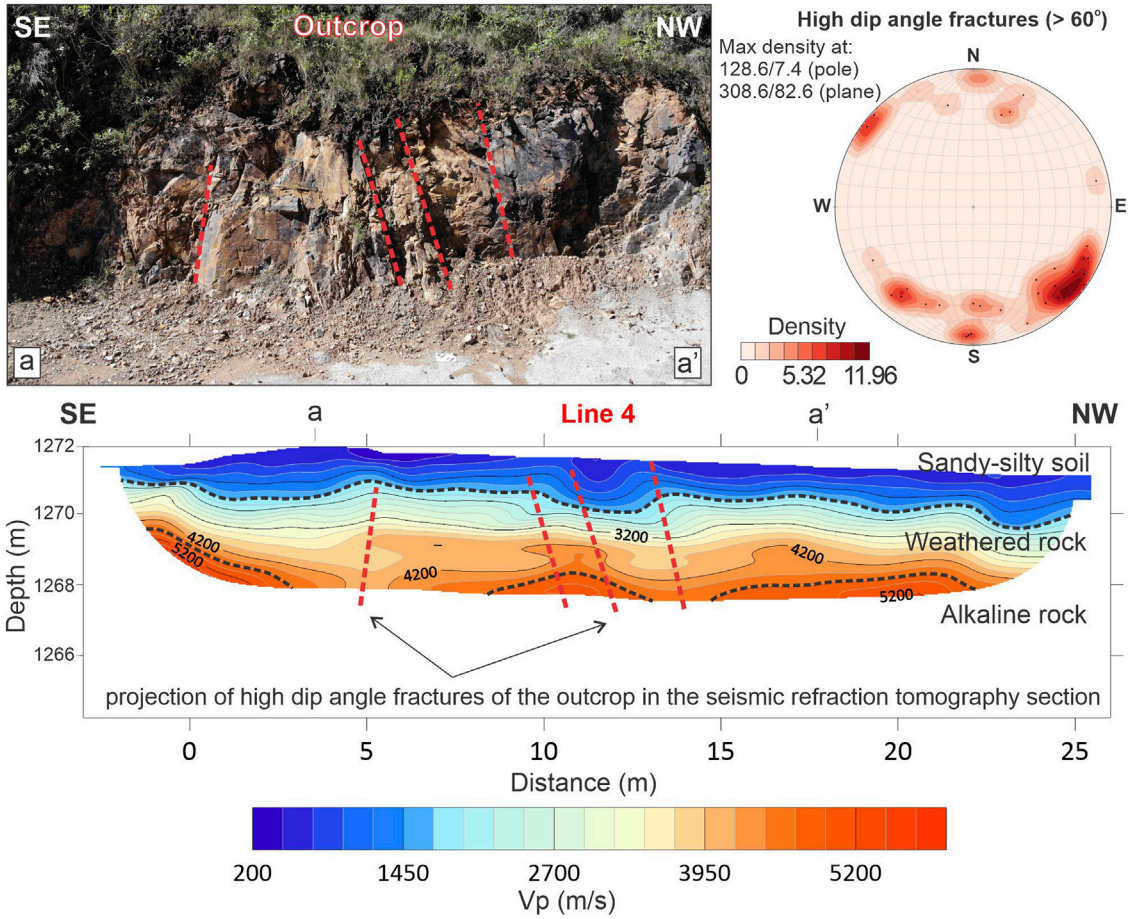

FIGURE 6
Structural survey and seismic refraction in the outcrop of rock mass from Line 4. Fractures with high dip angle in the outcrop are traced in red.

5.2 Bedrock fracture strikes and the results of seismic refraction tomography

Seismic methods generate elastic waves that propagate in the physical environment (Schuck and Lange, 2007). Elastic waves are driven by strain energy pulses and have distinct speeds and propagation modes in solid and fluid media (Carcione et al., 2018). The propagation of seismic waves underground is directly related to the geology (Stokoe and Santamarina, 2000; Foti, 2005). The lithology, controlled by its mineralogical composition, is influenced by the degree of compaction, cementation, amount of clay, and disposition and texture of the grains, all of which will affect the propagation of seismic waves (Khandelwal, 2012). Other factors such as the degree of alteration and fracturing of the rock also influence the propagation of seismic waves (Berryman, 2007; Lei, 2022). The result from seismic data is an image of the subsurface, which can include geological layers and stratigraphic variations, top of bedrock, and the water level, for example, (Schuck and Lange, 2007; Stark, 2008).

The bedrock fracture strike measurements were fundamental to interpreting the seismic refraction tomography (SRT). The SRT performed on the outcrop near the foot of the dam shows three Vp layers (Figure 6). The most superficial layer, with Vp values up to 1,700 m/s, is consistent with the typical soil found in drillings carried out in the area (marked by the dashed black line in Figure 6). The soil layer is about a meter thick. Under the soil layer, higher values of Vp are observed that vary between 2,700 m/s and 5,400 m/s and are consistent with the values of rock masses (Capizzi and Martorana, 2014; Tomás et al., 2018). The historical geological mapping in the mining area (mine pit and pre-installation of the dam) indicated the presence of rock at 1,271 m. Different degrees of alteration were mapped in this mine pit area and resulted in different rock quality designations (Instituto de Pesquisas Tecnológicas – IPT, 1977; Fraenkel et al., 1985). The main factor related to the different degrees of alteration was the variations of the degrees of fracturing. Fracturing facilitates the flow of water in the rock and thus alteration and variation in the seismic velocity values. Results of the seismic refraction tomography showed variations of Vp values precisely at the depths associated with the presence of weathered rock (Figure 6).

The seismic results obtained in the outcrop area were compared with the visual fractures observed in the field. The position of fractures in outcrop matched vertical seismic anomalies in the SRT section (a-a'; Figure 6). The layer with Vp values of 3,950 m/s, interpreted as weathered rock in the study and supported by geological drillings carried out in the area, showed

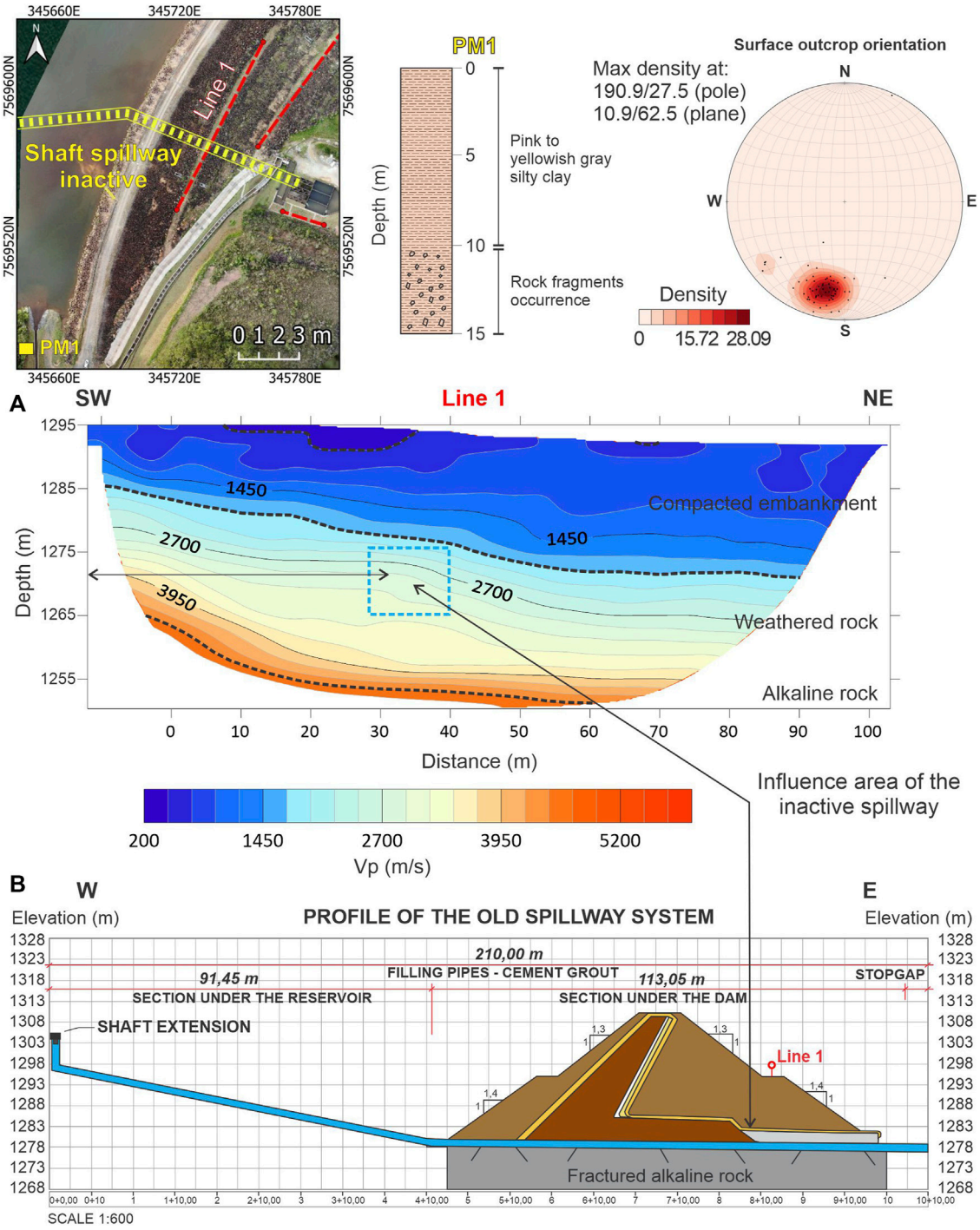

FIGURE 7
(A) Results of seismic refraction obtained in Line 1 of dam body, geological description of cuttings from a borehole and structural survey. **(B)** Profile of the inactive shaft spillway on Line 1 and the seismic refraction result.

an increase in thickness close to the position of the fractures (Figure 6). This result suggests that fractures may facilitate the percolation of water inside the rock, and that alteration of the rock by chemical weathering results in decreased seismic wave velocity values. In dams that store radioisotopes, as is the case of the present study, mapping fractures via seismic helps us to map preferential pathway and thus possible contamination. Although it is not possible to confirm the percolation of contaminants with geophysics alone, the identification of the different degrees of fracturing of the rock may help in siting groundwater monitoring wells where geochemical tests to explore leakage scenarios could be conducted.

The seismic refraction tomography results obtained in the lines made in the body of the dam downstream showed Vp values

consistent with the materials used for the construction of the dam. Line 1, performed on the highest berm (first berm; Figure 1A) and farther away from the rock mass, showed shallow Vp values up to 1,700 m/s, associated with the compacted soil of the dam body. Increases in Vp values were also observed with increasing depth until reaching a value close to 5,200 m/s, consistent with the less weathered rock (Figure 7). Due to the topographic variation of the terrain, there was an increase in the thickness of the bedrock as there was a separation of the region of contact of the abutment with the natural relief. The orientation of the seismic layer was consistent with the outcrop surface direction and angle of dip. This interpretation was corroborated by cuttings from a borehole located on the right abutment of the dam. At a depth of 10 m, fragments of rock were observed in this well (Figure 7A). The identification in this variability in thickness may assist in the construction of geological-geotechnical models in monitoring studies of such engineering projects.

5.3 Location of inactive hydraulic structures in the dam foundation

An anomalous response was identified in Line 1 between the distances of 30 m and 35 m in the seismic refraction tomography section (rectangle in blue in Figure 7A). The seismic layer at this location widened and curved. After the 40 m position in the seismic refraction tomography section, the strata returned to horizontal. Through the historical record of the operational and maintenance activities carried out on the dam, it was observed that at this point the old spillway, currently deactivated, crossed the section horizontally and in depth (Figure 7B). Identification of the presence and positioning of a hydraulic structure within the body or foundation of dams through non-invasive methodologies is desirable in dam maintenance studies. The deterioration process of internal structures, such as gates and valves, as well as the presence of erosion in the foundation, can compromise the stability of the dam. The lack of maintenance of the hydraulic structure can lead to leaks, infiltrations, and slides, triggering dam failure and jeopardizing adjacent communities and environmental resources. The hydraulic structure was filled with cement, so the elastic differences between the cement and rock were sufficient to cause variations in the seismic velocity. In civil engineering, soil and rock-concrete interfaces are generally considered potentially vulnerable zones. Deformation and failure can easily appear at these interfaces, progress under various loads, and induce engineering safety risks such as shear failure and risk of structure slippage (Jiang et al., 2021).

The seismic response related to the presence of the hydraulic structure at this depth showed that the acquisition was capable of identifying small changes in the composition of the material inside the dam associated with the elastic changes of the different materials. The section with the quantity of seismic rays in Line 1 exhibited an anomalous behavior similar to the behavior of Line 3 (Supplementary Figure S8), which will be presented next. In both cases, hydraulic elements (inactive spillway) and geological elements (boulders) were identified at these depths and influenced the behavior of seismic waves in the medium. This behavior was not observed in the results of Line 2, for example, which did not show peak values in seismic rays at specific depths. The distribution of seismic rays at depth showed a considerable number of seismic rays even at 1,277 m, below the location of the inactive drainage system (Supplementary Figure S8). The results of the seismic refraction tomography did not identify anomalies under the depth of the rock-concrete interfaces, which are the inactive concrete spillway and the bedrock. It is not possible to affirm that there are no deformations in this contact; however, the distribution of seismic rays at depth showed a considerable number of seismic rays even at 1,277 m, below the location of the inactive drainage system (Supplementary Figure S8), which supports this conclusion.

5.4 Possible influence of the saturated-sand filter on the propagation of the compressional wave

Line 2, carried out on the lowest berm (2ª berm; Figure 1A) and close to the rock mass, also showed results consistent with the typical section of the dam (Figure 8). Between the distances of 0-15 m, the SRT section shows a horizontal seismic layer with no large variations in the Vp values and values consistent with weathered rock. At distances of 20 m and 35 m, according to the section of the dam, a 4-m thick saturated-sand filter was installed to release water at a depth of 9 m. This horizontal structure is composed of sand and observed in the SRT. Seismic strata with Vp values close to 1,450 m/s and 1,700 m/s showed increased thickness at this depth (Figure 8).

It was not possible to state that the observed seismic anomalies are related only to the presence of the saturated filter or physical changes in the material of the contact zone between the dam body and the rock foundation, such as compaction deficiencies. The vertical seismic anomalies observed in line 2 did not have the same pattern as the anomalies interpreted in the seismic refraction tomography section of the outcrop. The seismic response with values greater than 5,200 m/s from the elevation of 1,260 m, interpreted as alkaline rock, did not show vertical anomalies as were seen in the results observed in the seismic tests of the outcrop. Regardless, the identification of altered areas in the contact between the body and the foundation of the dam that may compromise the physical integrity of the structure are important in monitoring of the dam at this interface (compacted soil and rock foundation), which is important for the stability of the structure.

5.5 Presence of boulders in the dam's foundation and the refraction seismic response

The acquisition line located at the foot of the downstream slope (Line 3; Figure 1A) was carried out in an area with a thin layer of soil. Among all the acquisition lines performed, Line 3 is the closest to the alkaline rock. During data acquisition, the presence of rock blocks of different dimensions between the foot of the dam and the natural relief (left abutment) was observed (white arrows in Figure 9), and these rock blocks were identified in the SRT near an elevation of 1,260 m with Vp values between 3,250 m/s and 3,950 m/s (Figure 9).

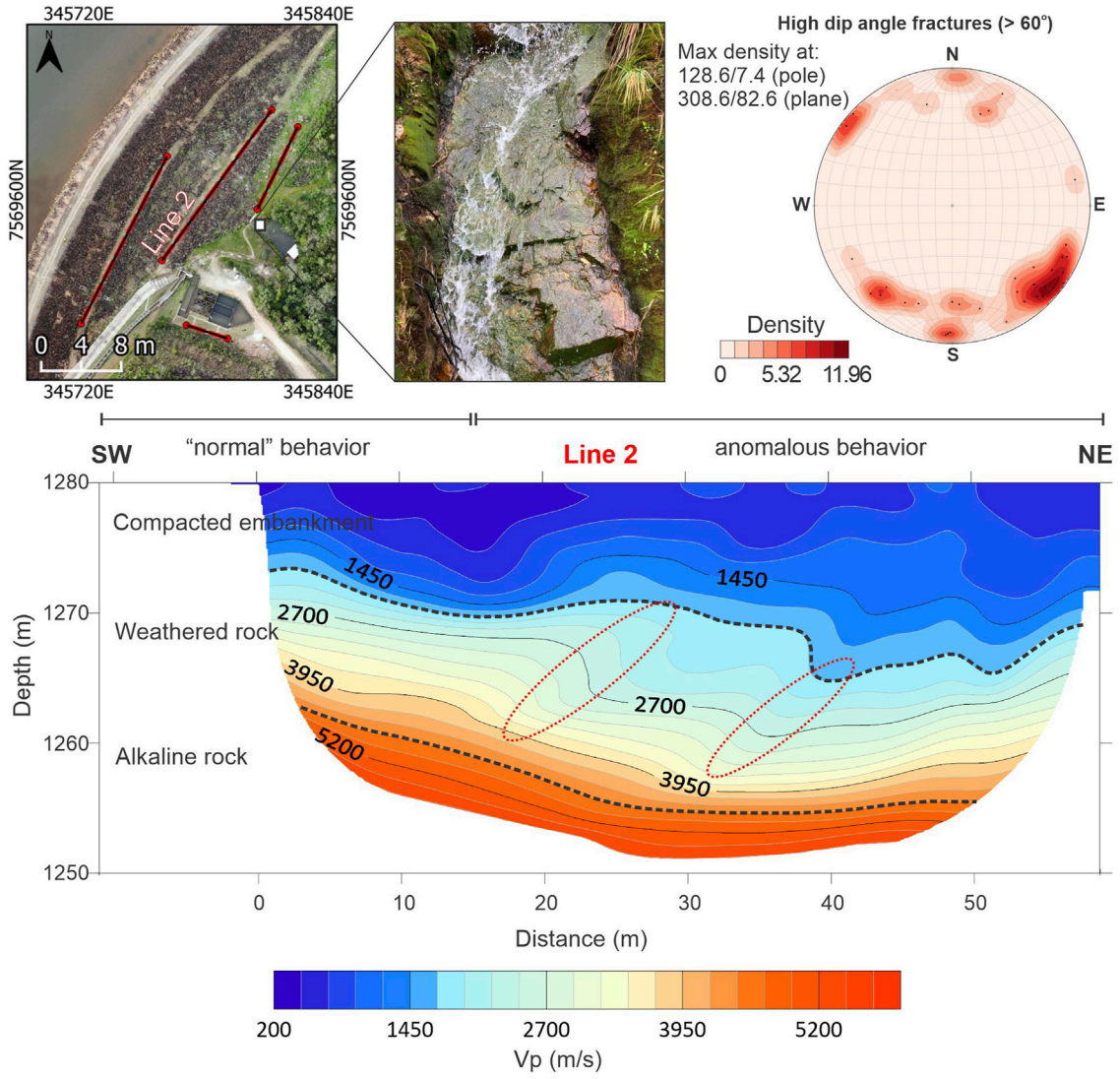

FIGURE 8
Results obtained in Line 2 of the dam body with anomalous behavior highlighted in red.

The presence of rock blocks near the rock mass of the dam foundation is not desirable in dam engineering projects; they are considered defective materials in the rock massif. In the present study, the rock blocks are arranged between the compacted soil layer and weathered rock, and may influence the compaction of the material and act as a facilitating agent in the development of preferential water flow paths. The layer with Vp values of 3,950 m/s, consistent with weathered rock, showed an increase in thickness in the contact of the dam and the natural relief (Figure 9), which might suggest possible saturation, water flow, or material alteration.

6 Conclusion

The environmental liabilities arising from mining activity are diverse. Mining tailings storage structures need to be monitored and investigated for physical integrity. Geophysical methods provide non-invasive ways to extrapolate beyond the traditional geotechnical instruments applied in dams. The integration of the different methodologies proposed allowed us to analyze the feasibility of using structural mapping by photogrammetry and to compare this mapping with the results from seismic refraction to observe increases in fracturing in the dam foundation mass. The methodology presented here can be applied to other dams and tailings piles to map zones of concern from alteration of the rock mass of the foundation to positioning of fractures. In our work, we found that.

(1) The strike of fractures obtained indirectly from the UAV showed greater variability than the compass-based measurements. However, the maximum fracture density estimated was similar for both measurements. This result shows the potential reliability and utility of UAV-based monitoring of rock masses in environments at risk of human exposure such as massifs of mining slopes with risk of falling blocks or dams with high risk of rupture.

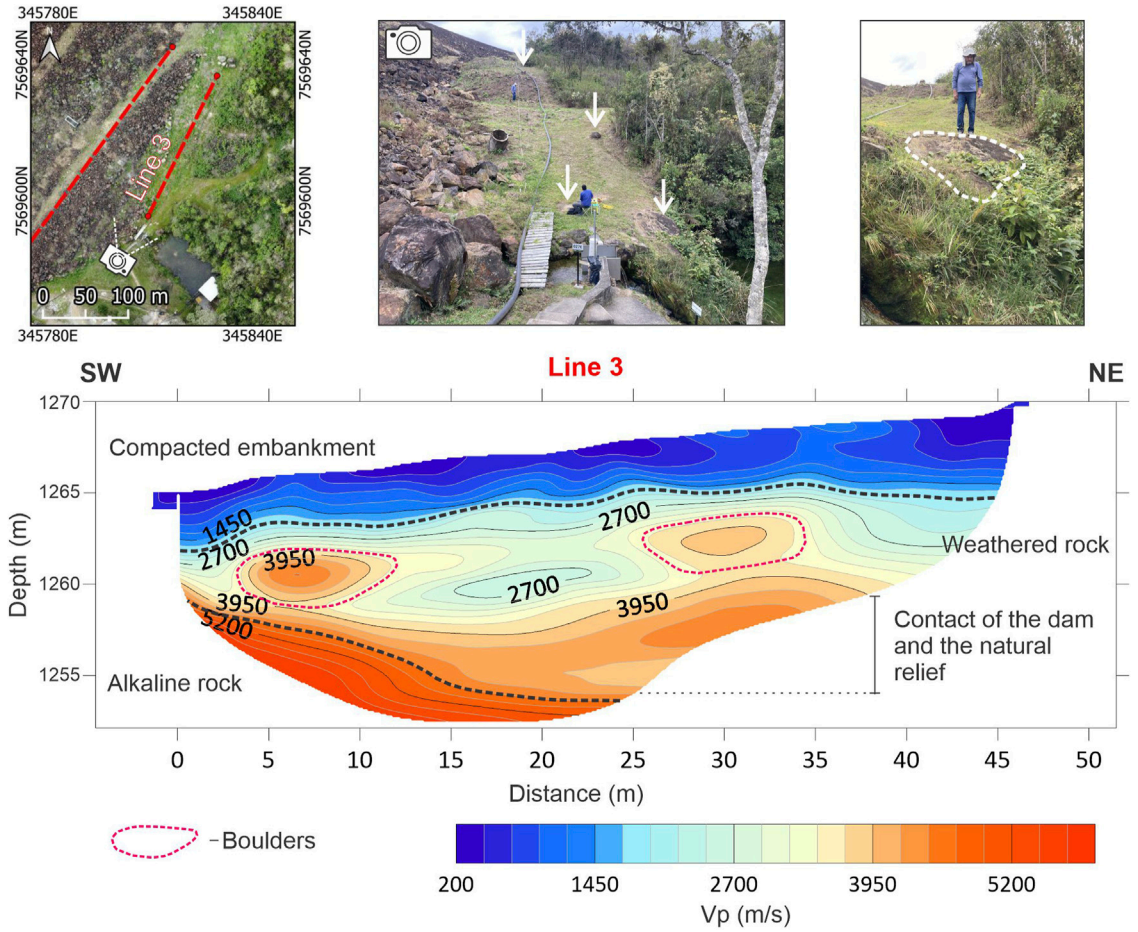

FIGURE 9
Results obtained at the foot of the slope downstream of the dam on Line 3. Two anomalies can be seen near a depth of 5 m.

(2) The seismic results obtained in the rock mass outcrop near the foot of the dam (Line 4) showed vertical, linear anomalies consistent with the positioning of the high dip-angle fracture family, although it was not sensitive variations from the family of low-angle fractures. However, in one of the lines made on the dam's berm (Line 1), the dip angle of the seismic stratum was consistent with the direction and angle of dip of the bedrock in the study region. The visualization of fracturing of the foundation rock mass may help in the identification of leaks. This information is crucial for decision-making in environmental monitoring and recovery projects.

(3) In all SRT sections performed on the body and foot of the dam (Lines 2 and 3), variations in depth were observed linked to the degree of fracturing of the rock, and we additionally mapped an inactive spillway and blocks of rock at the foot of the dam that could compromise the physical integrity of the dam. The results can assist in the construction of geological-geotechnical models in engineering studies.

(4) Seismic refraction, although not commonly applied in dam engineering studies, is a non-invasive alternative to assess the degree of fracturing of rock masses of dam foundations consistent with corrobatory measurements. In addition to mapping the degree of fracturing it had utility in identifying hydraulic structures and geological elements, specifically inactive spillways and rock blocks. The identification of hydraulic and geological structures that alter the physical integrity of the dam without the need for invasive investigations that might alter the compaction of the materials in the dam body are important, especially in dams and tailings piles that present a high risk of rupture.

Data availability statement

The datasets presented in this study can be found in online repositories. The names of the repository/repositories and accession number(s) can be found below: https://www.hydroshare.org/resource/1db2d58d3bb24eaca5eaca0ff761fda2/.

Author contributions

LN: Conceptualization, Data curation, Investigation, Methodology, Software, Writing–original draft, Writing–review and editing. KS: Data curation, Supervision, Writing–original draft, Writing–review and editing. CM: Funding acquisition, Investigation, Project administration, Supervision, Writing–review

and editing. OG: Investigation, Methodology, Writing–review and editing. DA: Data curation, Software, Writing–review and editing.

Funding

The author(s) declare financial support was received for the research, authorship, and/or publication of this article. The authors thank the São Paulo Research Foundation (FAPESP) for the financial support whereby process number 2020/14647-0 (Regular Project) and the National Council for Scientific and Technological Development (CNPq) for financial support in the granting of a sandwich doctoral scholarship for the execution of activities abroad under process number 201030/2022-5.

Acknowledgments

The authors thank the Brazilian Nuclear Industries for allowing access to the study area and providing technical and operational support during the studies and Institute for Technological Research for technical support during data acquisition activities.

Conflict of interest

The authors declare that the research was conducted in the absence of any commercial or financial relationships that could be construed as a potential conflict of interest.

Publisher's note

Supplementary material

The Supplementary Material for this article can be found online at: https://www.frontiersin.org/articles/10.3389/feart.2023.1281076/full#supplementary-material

References

Albarelli, D. S. N. A., Mavrouli, O. C., and Nyktas, P. (2021). Identification of potential rockfall sources using UAV-derived point cloud. *Bull. Eng. Geol. Environ.* 80, 6539–6561. doi:10.1007/s10064-021-02306-2

Almeida, F. F. M. (1986). Distribuição regional e relações tectônicas do magmatismo pós-paleozoico no Brasil. *Rev. Bras. Geociênc* 16, 325–349. doi:10.25249/0375-7536.1986325349

Almeida Filho, R., and Paradella, W. R. (1977). *Estudo do maciço alcalino de Poços de Caldas através de imagens Landsat com ênfase em mineralizações radioativas*. Dissertação de mestrado. Instituto Nacional de Pesquisas Espaciais (INPE), São José dos Campos, SP.

Arcila, E. J. A., Moreira, C. A., Camarero, P. L., and Casagrande, M. F. S. (2021). Identification of flow zones inside and at the base of a uranium mine tailings dam using geophysics. *Mine Water Environ.* 40, 308–319. doi:10.1007/s10230-020-00746-y

Association of State Dam Safety Officials – ASDSO (2023). Dam safety incident database search. Association of state dam safety Officials website. Accessed in May, 2023 Available at: https://damsafety.org/Incidents.

Asthana, B. N., and Khare, D. (2022). *Recent advances in dam engineering. Recent advances in dam engineering*. Springer International Publishing, 366p.

Bedrosian, P. A., Burton, B. L., Powers, M. H., Minsley, B. J., Phillips, J. D., and Hunter, L. E. (2012). Geophysical investigations of geology and structure at the martis creek dam, truckee, California. *J. Appl. Geophys* 77, 7–20. doi:10.1016/j.jappgeo.2011.11.002

Benjumea, B., Gabàs, A., Macau, A., Ledo, J., Bellmunt, F., Figueras, S., et al. (2021). Undercover karst imaging using a Fuzzy c-means data clustering approach (Costa Brava, NE Spain). *Eng. Geol.* 293, 106327. doi:10.1016/j.enggeo.2021.106327

Berryman, J. G. (2007). Seismic waves in rocks with fluids and fractures. *Geophys J. Int.* 171 (2), 954–974. doi:10.1111/j.1365-246X.2007.03563.x

Biondi, J. C. (1976). "Cubagem e avaliação do depósito de urânio do Cercado (c -09)," in *Relatório interno NUCLEBRÁS* (Rio de Janeiro, RJ.

Camarero, P. L., Moreira, C. A., and Pereira, H. G. (2019). Analysis of the physical integrity of earth dams from electrical resistivity tomography (ERT) in Brazil. *Pure Appl. Geophys.* 176, 5363–5375. doi:10.1007/s00024-019-02271-8

Camarero, P. L., Moreira, C. A., Targa, D. A., Duz, B. G., and Pereira, H. G. (2021). Analysis of acid drainage flow zones in a rocky massif in a uranium mine from structural and geophysical diagnoses. *Mine Water Environ.* 41, 303–316. doi:10.1007/s10230-021-00827-6

Capizzi, P., and Martorana, R. (2014). Integration of constrained electrical and seismic tomographies to study the landslide affecting the cathedral of Agrigento. *J. Geophys Eng.* 11 (4), 045009. doi:10.1088/1742-2132/11/4/045009

Carcione, J. M., Bagaini, C., Ba, J., Wang, E., and Vesnaver, A. (2018). Waves at fluid–solid interfaces: explicit versus implicit formulation of the boundary condition. *Geophys J. Int.* 215 (1), 37–48. doi:10.1093/gji/ggy262

Cardarelli, E., Cercato, M., and De Donno, G. (2014). Characterization of an earth-filled dam through the combined use of electrical resistivity tomography, P- and SH-wave seismic tomography and surface wave data. *J. Appl. Geophys* 106, 87–95. doi:10.1016/j.jappgeo.2014.04.007

Chen, Y., Wang, S., Ren, W., Yang, Z., Hu, R., and Mao, Y.-P. (2023). Detection of leakage in the plunge pool area at Xiluodu arch dam with an integrated approach. *J. Hydrol.* 618, 129135. doi:10.1016/j.jhydrol.2023.129135

Cipriani, M. (2002). *Mitigação dos Impactos Sociais e Ambientais Decorrentes do Fechamento Definitivo de Minas de Urânio*. Campinas: Tese de Doutorado - Universidade Estadual de Campinas - Instituto de Geociências, 332.

Dimech, A., Cheng, L., Chouteau, M., Chambers, J., Uhlemann, S., Wilkinson, P., et al. (2022). A review on applications of time-lapse electrical resistivity tomography over the last 30 Years: perspectives for mining waste monitoring. *Surv. Geophys* 43, 1699–1759. doi:10.1007/s10712-022-09731-2

Eidemüller, D. (2021). *Economic, Ecological and Political Aspects of Nuclear Energy. In: Nuclear Power Explained. Springer Praxis Books (POPS)*. Springer, Cham. doi:10.1007/978-3-030-72670-6_7

Fell, R., MacGregor, P., Stapledon, D., and Bell, G. (2005). *Geotechnical engineering of dams*. CRC Press, 930. doi:10.1201/NOE0415364409

Filho, C. A. C. (2014). *Avaliação da qualidade das águas superficiais no entorno das instalações minero-industriais de urânio de Caldas*. Belo Horizonte, 341. Tese de doutorado – Comissão Nacional de Energia Nuclear, Centro de Desenvolvimento da Tecnologia Nuclear. Available at: https://sucupira.capes.gov.br/sucupira/public/consultas/coleta/trabalhoConclusao/viewTrabalhoConclusao.jsf?popup=true&id_trabalho=2102763

Foti, S., Hollender, F., Garofalo, F., Albarello, D., Asten, M., Bard, P.-Y., et al. (2018). Guidelines for the good practice of surface wave analysis: a product of the InterPACIFIC project. *Bull. Earthq. Eng.* 16, 2367–2420. doi:10.1007/s10518-017-0206-7

Foti, S., Sambuelli, L., Socco, V. L., and Strobbia, C. (2003). Experiments of joint acquisition of seismic refraction and surface wave data. *Near Surf. geophys* 1 (3), 119–129. doi:10.3997/1873-0604.2003002

Foti, S. (2005). *Surface Wave Testing for Geotechnical Characterization*. Editor C. G. Lai and K. Wilmański (Springer, Vienna: Surface Waves in Geomechanics: Direct and Inverse Modelling for Soils and Rocks. CISM International Centre for Mechanical Sciences) 481. doi:10.1007/3-211-38065-5_2

Fraenkel, M. O., Santos, R. C., Loureiro, F. E. V. L., and Muniz, W. S. (1985). "Jazida de urânio no planalto de Poços de Caldas, Minas Gerais," in *Principais depósitos minerais do Brasil, DNPM/CVRD*. Editors C. Schobbenhaus and C. E. S. Coelho, Brasília (coords, I), 89–103.

Geração controlada com destinação segura disposição total a seco (2019). Geração controlada com destinação segura disposição total a seco - barragens e seus sistemas de

gestão e tendências para o tratamento, disposição e reaproveitamento de rejeitos e resíduos. *Inthemine* 14. 19–26. (Especial rejeitos).

Grohmann, C., and Campanha, G. (2010). *OpenStereo: open source, cross-platform software for structural geology analysis*. American Geophysical Union.

Guedes, V. J. C. B., Borges, W. R., da Cunha, L. S., and Maciel, S. T. R. (2023). Characterization of an earth dam in Brazil from seismic refraction tomography and multichannel analysis of surface waves. *J. Appl. Geophys* 208, 104893. doi:10.1016/j.jappgeo.2022.104893

Guireli Netto, L., Gandolfo, O. C. B., Malagutti Filho, W., and Dourado, J. C. (2020b). Non-destructive investigation on small earth dams using geophysical methods: seismic surface wave multichannel analysis (MASW) and S-wave refraction seismic methods. Braz J Geophys, *[S.l.]* 38 (1), 5–19. doi:10.22564/rbgf.v38i1.2031

Guireli Netto, L., Malagutti Filho, W., and Gandolfo, O. C. B. (2020a). Detection of seepage paths in small earth dams using the self-potential method (SP). *Int. Eng. J.* 73, 303–310. doi:10.1590/0370-44672018730168

Guo, Y., Cui, Y. A., Xie, J., Luo, Y., Zhang, P., Liu, H., et al. (2022). Seepage detection in earth-filled dam from self-potential and electrical resistivity tomography. *Eng. Geol.* 306, 106750. doi:10.1016/j.enggeo.2022.106750

Habel, M., Mechkin, K., Podgorska, K., Saunes, M., Babiński, Z., Chalov, S., et al. (2020). Dam and reservoir removal projects: a mix of social-ecological trends and cost-cutting attitudes. *Sci. Rep.* 10, 19210. doi:10.1038/s41598-020-76158-3

Instituto de Pesquisas Tecnológicas – IPT (1977). *A" e "B" - mina do Cercado (Poços de Caldas, MG)*. São Paulo. (Relatório no 10.142).Ensaios geofísicos (sísmica de refração e eletrorresistividade) para detalhamento das características físicas gerais das rochas que ocorrem sobre os corpos de minério

Islam, K., and Murakami, S. (2021). Global-scale impact analysis of mine tailings dam failures: 1915–2020. *Glob. Environ. Chang.* 70, 102361. doi:10.1016/j.gloenvcha.2021.102361

Jansen, R. B. (1983). *Dams and public safety*. Denver: A Water Resources Technical Publication, U.S. Department of the Interior, Bureau of Reclamation.

Jiang, Q., Yang, Y., Yan, F., Zhou, J., Li, S., Yang, B., et al. (2021). Deformation and failure behaviours of rock-concrete interfaces with natural morphology under shear testing. *Constr. Build. Mater.* 293, 123468. doi:10.1016/j.conbuildmat.2021.123468

Junaid, M., Abdullah, R. A., Sa'ari, R., Rehman, H., Shah, K. S., Ullah, R., et al. (2022). Quantification of rock mass condition based on fracture frequency using unmanned aerial vehicle survey for slope stability assessment. *J. Indian Soc. Remote Sens.* 50, 2041–2054. doi:10.1007/s12524-022-01578-9

Khandelwal, M. (2012). Correlating P-wave velocity with the physico-mechanical properties of different rocks. *Pure Appl. Geophys* 170, 507–514. doi:10.1007/s00024-012-0556-7

Kirchherr, J., and Charles, K. (2016). The social impacts of dams: a new framework for scholarly analysis. *Environ. Impact Assess. Rev.* 60, 99–114. doi:10.1016/j.eiar.2016.02.005

Koppe, J. C. (2021). Lessons learned from the two major tailings dam accidents in Brazil. *Mine Water Environ.* 40, 166–173. doi:10.1007/s10230-020-00722-6

Lecomte, I., Gjøystdal, H., Dahle, A., and Pedersen, O. C. (2000). Improving modelling and inversion in refraction seismics with a first-order Eikonal solver. *Geophys Prospect* 48, 437–454. doi:10.1046/j.1365-2478.2000.00201.x

Lei, Q. (2022). Impact of fracture normal and shear stiffnesses on the scattering attenuation of P and S waves in a naturally fractured rock. *J. Appl. Geophys* 206, 104784. doi:10.1016/j.jappgeo.2022.104784

Liu, K., Yuan, W., and Wang, Y. (2021). "Influence of heterogeneity on the elastic contact problems in geotechnical engineering," in *Challenges and innovations in geomechanics. IACMAG 2021. Lecture notes in civil engineering*. Editors M. Barla, A. Di Donna, and D. Sterpi (Cham: Springer), 125. doi:10.1007/978-3-030-64514-4_104

Lottermoser, B. G. (2010). "Mine wastes," in *characterization, treatment and environmental impacts*. third edition (Springer), 1–400.

Maalouf, Y., Bièvre, G., Voisin, C., and Khoury, N. (2022). Geophysical monitoring of a laboratory scale internal erosion experiment. *Near Surf. Geophys* 20, 365–383. doi:10.1002/nsg.12215

Magno Júnior, L. B. (1985). "Osamu Utsumi mine, geologic presentation," in *Relatório interno NUCLEBRÁS* (Rio de Janeiro, RJ.

Moreira, C. A., Guireli Netto, L., Camarero, P. L., Bertuluci, F. B., Hartwig, M. E., and Domingos, R. (2022). Application of electrical resistivity tomography (ERT) in uranium mining earth dam. *J. Geophys Eng.* 19 (6), 1265–1279. doi:10.1093/jge/gxac082

Mundeli, R. M., and Shirabe, T. (2021). An experimental analysis of least-cost path models on ordinal-scaled raster surfaces. *Int. J. Geogr. Inf. Sci.* 35 (8), 15 45–1569. doi:10.1080/13658816.2020.1753204

Nesbit, P. R., Durkin, P. R., Hugenholtz, C. H., Hubbard, S. M., and Kucharczyk, M. (2018). 3-D stratigraphic mapping using a digital outcrop model derived from UAV images and structure-from-motion photogrammetry. *Geosphere* 14 (6), 2469–2486. doi:10.1130/GES01688.1

Oliveira, L., Braga, M. A., Prosdocimi, G., Cunha, A., Dias, L., and Gama, F. (2023). Improving tailings dam risk management by 3D characterization from resistivity tomography technique: case study in São Paulo – Brazil. *J. Appl. Geophys* 210, 104924. doi:10.1016/j.jappgeo.2023.104924

Owen, J. R., Kemp, D., Lèbre, É., Svobodova, K., and Murillo, G. P. (2020). Catastrophic tailings dam failures and disaster risk disclosure. *Int. J. Disaster Risk Reduct.* 42, 101361. doi:10.1016/j.ijdrr.2019.101361

Rotta, L. H. S., Alcântara, E., Park, E., Negri, R. G., Lin, Y. N., Bernardo, N., et al. (2020). The 2019 Brumadinho tailings dam collapse: possible cause and impacts of the worst human and environmental disaster in Brazil. *Int. J. Appl. Earth Obs. Geoinf* 90, 102119. doi:10.1016/j.jag.2020.102119

Salvini, R., Mastrorocco, G., Seddaiu, M., Rossi, R., and Vanneschi, C. (2017). The use of an unmanned aerial vehicle for fracture mapping within a marble quarry (Carrara, Italy): photogrammetry and discrete fracture network modelling. *Geomatics, Nat. Hazards Risk* 8 (1), 34–52. doi:10.1080/19475705.2016.1199053

Sari, M., Seren, A., and Alemdag, S. (2020). Determination of geological structures by geophysical and geotechnical techniques in Kırklartepe Dam Site (Turkey). *J. Appl. Geophys* 182, 104174. doi:10.1016/j.jappgeo.2020.104174

Sastry, R. G., and Chahar, S. (2019). Geoelectric versus MASW for geotechnical studies. *J. Earth Syst. Sci.* 128, 34. doi:10.1007/s12040-018-1061-x

Schoenberger, E. (2016). Environmentally sustainable mining: the case of tailings storage facilities. *Resour. Policy* 49, 119–128. doi:10.1016/j.resourpol.2016.04.009

Schuck, A., and Lange, G. (2007). "Seismic methods," in *Environmental geology* (Berlin, Heidelberg: Springer). doi:10.1007/978-3-540-74671-3_11

Schuster, G. T., and Quintus-Bosz, A. (1993). Wavepath eikonal traveltime inversion; theory. *Geophys* 58 (9), 1314–1323. doi:10.1190/1.1443514

Schuster, R. L. (2006). *Interaction of dams and landslides—case studies and mitigation*, 1723. U.S. Geological Survey Professional Paper, 107. Available at: https://pubsdata.usgs.gov/pubs/pp/2006/1723/

Sentenac, P., Benes, V., Budinsky, V., Keenan, H., and Baron, R. (2017). Post flooding damage assessment of earth dams and historical reservoirs using non-invasive geophysical techniques. *J. Appl. Geophys* 146, 138–148. doi:10.1016/j.jappgeo.2017.09.006

Srivastava, H., Tiwari, R. P., Kumar, V., and Singh, D. (2023). "A review on various geotechnical and geophysical investigations for a dam rehabilitation project," in *Proceedings of Indian geotechnical and geoenvironmental engineering conference (IGGEC) 2021. Lecture notes in civil engineering*. Editors A. K. Agnihotri, K. R. Reddy, and H. S. Chore (Singapore: Springer), Vol. 280. 1. IGGEC 2021. doi:10.1007/978-981-19-4739-1_8

Stark, A. (2008). *Seismic methods and applications: a guide for the detection of geologic structures, earthquake zones and hazards, resource exploration, and geotechnical engineering*. Brown Walker Press, 592. Available at: https://books.google.com.br/books/about/Seismic_Methods_and_Applications.html?id=4G1-6l8ytnEC&redir_esc=y

Stokoe, K. H., and Santamarina, J. (2000). Seismic-wave-based testing in geotechnical engineering. *GeoEng*, 1490–1536.

Thiele, S. T., Grose, L., Samsu, A., Micklethwaite, S., Vollgger, S. A., and Cruden, A. R. (2017). Rapid, semi-automatic fracture and contact mapping for point clouds, images and geophysical data. *Solid earth.* 8, 1241–1253. doi:10.5194/se-8-1241-2017

Tomás, R., Abellán, A., Cano, M., Riquelme, A., Tenza-Abril, A. J., Baeza-Brotons, F., et al. (2018). A multidisciplinary approach for the investigation of a rock spreading on an urban slope. *Landslides* 15, 199–217. doi:10.1007/s10346-017-0865-0

Wang, Q., Guo, J., Li, R., and Jiang, X. (2023). Is nuclear power a cost-effective energy transition option? Comparative study on the impact of coal, oil, gas, renewable and nuclear power on economic growth and carbon emissions. *Environ. Res.* 221, 115290. doi:10.1016/j.envres.2023.115290

Wu, H., Chen, J., Xu, J., Zeng, G., Sang, L., Liu, Q., et al. (2019). Effects of dam construction on biodiversity: a review. *J. Clean. Prod.* 221, 480–489. doi:10.1016/j.jclepro.2019.03.001

Xuhua, R., Jiaqing, S., Nenghui, B., and Hongyun, R. (2008). Stability analysis of concrete gravity dam on complicated foundation with multiple slide planes. *Water Sci. Eng.* 1. doi:10.3882/j.issn.1674-2370.2008.03.007

Yemel'yanov, V. S., and Yevstyukhin, A. I. (1969). *The Metallurgy of Nuclear Fuel*. Pergamon, Properties and Principles of the Technology of Uranium, Thorium and Plutonium, Page iii. doi:10.1016/B978-0-08-012073-7.50002-8

Zelt, C. A., Haines, S., Powers, M. H., Sheehan, J., Rohdewald, S., Link, C., et al. (2013). Blind test of methods for obtaining 2-D near-surface seismic velocity models from first-arrival traveltimes. *J. Environ. Eng. Geophys* 18 (3), 183–194. doi:10.2113/JEEG18.3.183

Zhang, B., Wang, J. G., and Shi, R. (2004). Time-dependent deformation in high concrete-faced rockfill dam and separation between concrete face slab and cushion layer. *Comput. Geotech.* 31, 559–573. doi:10.1016/j.compgeo.2004.07.004

Zhang, L., Peng, M. C., and Dongsheng X, Y. (2016). *Dam failure mechanisms and risk assessment - 4.3 common causes of concrete dam failures*. John Wiley and Sons. Available at: https://app.knovel.com/hotlink/pdf/id:kt011HHO92/dam-failure-mechanisms/common-causes-concrete.